Domain-specific DNA binding activities of BRCA1 reveal substrate preferences for homologous recombination and telomere regulation

*Kaitlin Lowran[1‡†], Laura Campbell[1‡§], Emma Cismas[1], and Colin G. Wu[1]**

[1] Department of Chemistry, Oakland University, Rochester, MI, 48309, USA

*Email: colinwu@oakland.edu

‡ K.L. and L.C. contributed equally to this paper.

ABSTRACT

BRCA1 is a crucial mediator of homologous recombination (HR), a high-fidelity pathway for repairing double-stranded DNA breaks (DSBs) in human cells. The central region of BRCA1 protein contains two putative DNA binding domains (DBDs), yet their relative substrate specificities and functional contributions to HR remain unclear. Here, we characterized the DNA binding properties of DBD1 (amino acids 330-554), DBD2 (amino acids 894-1057), and the BRCA1 C-terminal (BRCT) repeats using biolayer interferometry. We assessed their affinities for single-stranded DNA (ssDNA), double-stranded DNA (dsDNA), and G-quadruplex (G4) structures. DBD1 exhibited the highest affinity for dsDNA, while DBD2 and BRCT bound preferentially to ssDNA and G4. These findings support a model in which DBD1 directs BRCA1 to DSB sites to facilitate DNA end resection during HR, whereas DBD2 and BRCT contribute to

19 the role of BRCA1 in telomere maintenance and chromatin remodeling through the recognition of
20 non-canonical DNA structures.

21 **INTRODUCTION**

22 The Breast Cancer Susceptibility Gene 1 (*BRCA1*) encodes a large tumor suppressor protein that
23 is essential for maintaining genomic integrity. BRCA1 plays pivotal roles in the repair of double-
24 stranded DNA breaks (DSB), transcriptional regulation, and telomere maintenance (1-4).
25 Germline mutations in *BRCA1* are associated with elevated risks of breast and ovarian cancers, as
26 well as cardiovascular diseases (5, 6). BRCA1 facilitates DSB repair during homologous
27 recombination (HR) by coordinating the recruitment of DNA end-resection proteins such as 53BP1
28 (3, 7, 8). This is subsequently followed by interaction with PALB2 to promote BRCA2/RAD51-
29 mediated strand invasion (9-11). Additionally, BRCA1 stabilizes stalled replication forks and
30 promotes recovery during replication stress (12, 13).

31 Replication stress arises from obstacles such as DNA damage, common fragile sites, and non-
32 canonical DNA structures (14). If left unresolved, these impediments can lead to fork collapse and
33 the formation of DSB, which must be efficiently repaired to prevent genomic instability and
34 tumorigenesis (15, 16, 17). While multiple DSB repair pathways exist—including non-
35 homologous end joining (NHEJ), alternative end joining, and single-strand annealing—HR is the
36 predominant mechanism and is favored for its high fidelity (18-21).

37 Non-canonical DNA structures, such as D-loops, cruciform, G-quadruplexes (G4), and other fork
38 intermediates, frequently arise during replication and transcription and must be properly resolved
39 to maintain genomic integrity (22). BRCA1 binds to several of these structures (23-26), a function

40 that may be relevant to its roles in telomere regulation and satellite DNA maintenance (2, 4, 27).
41 Notably, BRCA1-deficient cells are hypersensitive to G4-stabilizing compounds such as CX-5461,
42 which impedes replication fork progression and induces DNA breaks (28, 29).

43 Although BRCA1 is largely intrinsically disordered, it contains two well-characterized structured
44 domains: an N-terminal RING domain and a C-terminal BRCT domain. The RING domain forms
45 a heterodimer with the BARD1 tumor suppressor and functions as an E3 ubiquitin ligase (30-32).
46 The BRCA1-BARD1 complex binds preferentially to D-loops and DNA bubbles, facilitating
47 RAD51-mediated HR and replication fork restart at G4 regions (24, 33). In contrast, the BRCT
48 domain acts as a phospho-protein recognition site and is prevalent in other DNA repair proteins
49 (34). BRCA1 binds to the FANCJ helicase via the BRCT when FANCJ is phosphorylated on serine
50 990. Formation of the BRCA1-FANCJ complex may be needed for the conversion of interstrand
51 crosslinks (ICL) to DSB for repair by homologous recombination and to promote replication restart
52 at G4 sites (35-38). Beyond these roles, the BRCT domain also binds to supercoiled DNA,
53 contributes to chromatin remodeling, and participates in the detection of DNA breaks (39-42). It
54 also suppresses ribosomal R-loops by facilitating sense-antisense rRNA pairing and enhancing
55 RNA polymerase I-driven antisense rRNA transcription (43).

56 The central region of BRCA1, though unstructured, serves as a scaffold for protein and DNA
57 interactions (23, 26, 42, 44). Within this region, two discrete DNA binding domains (DBD) have
58 been identified: DBD1 (amino acids 330-554) and DBD2 (amino acids 894-1057) (40, 43, 45-47).

59 Although the relative affinities of the DBD for branched DNA substrates have been examined, the
60 results were mostly qualitative due to the presence of multiple BRCA1-DNA complexes (23). To
61 further characterize the DNA binding preferences of these domains, we have determined the

62 affinities of DBD1, DBD2, and BRCT for three DNA substrates representative of repair
63 intermediates: single-stranded DNA (ssDNA), double-stranded DNA (dsDNA), and G4 DNA. Our
64 findings suggest that the BRCA1 DBD are functionally specialized, with distinct substrate
65 specificities that may direct BRCA1 protein to either DSB or to the telomere during DNA damage
66 response.

67 **MATERIALS AND METHODS**

68 **Buffers and reagents.** All solutions were prepared with analytical-grade chemicals and Type I
69 ultrapure water from a Smart2Pure 6 UV/UF system (ThermoFisher; Waltham, MA, USA). The
70 solutions were then sterilized through a 0.22 µm PES filter prior to use.

71 **Expression and purification of recombinant proteins.** Codon-optimized *E. coli* expression
72 plasmids encoding human BRCA1 DBD1 (aa330-554), DBD2 (aa894-1057), and BRCT (aa1646-
73 1863) were purchased from VectorBuilder (Chicago, IL, USA). Constructs were transformed into
74 NiCo21(DE3) competent cells (New England Biolabs; Ipswich, MA, USA). Starter cultures (125
75 mL) were expanded into 4 L of LB medium (1:20 dilution) that was maintained at 37 °C and 250
76 rpm using a MaxQ 4000 orbital shaker (ThermoFisher). Protein expression was induced with 1
77 mM IPTG when the OD_{600} reached 0.6. After 4 hours of expression, the cells were harvested by
78 centrifugation using a J6-MI high-capacity centrifuge equipped with a JS-4.2 rotor (4,000 rpm at
79 4 °C for 90 minutes).

80 Cell pellets were resuspended in lysis buffer (20 mM NaPi (pH 7.5), 300 mM NaCl, 30 mM
81 imidazole, 1 mM DTT, 5% (v/v) glycerol, 1% NP-40, and 1 mM PMSF), and lysed by sonication
82 using a Fisherbrand 505 Dismembrator (Fisher Scientific; Hampton, NH, USA). Samples were
83 chilled on ice during sonication (15 seconds on, 45 seconds off, and 45% amplitude for 15

84 minutes). Lysates were clarified by centrifugation with a Sorvall RC5C Plus high-speed centrifuge
85 and a SS-34 fixed angle rotor (18,500 rpm at 4 °C for 90 minutes). The supernatant was filtered
86 through a 0.45 µm PES membrane prior to liquid chromatography.

87 All protein purification steps were performed at 4 °C. Clarified lysates were incubated for 45
88 minutes with 20 mL Ni-NTA agarose resin (Goldbio; St. Louis, MO, USA) that was pre-
89 equilibrated in binding buffer (20 mM NaPi (pH 7.5), 300 mM NaCl, 30 mM imidazole, 1 mM
90 DTT, and 5% glycerol). After batch binding, the resin was washed sequentially with 10 column
91 volumes (CV) of equilibration buffer and 10 CV of low-salt buffer (20 mM NaPi (pH 7.5), 30 mM
92 NaCl, 30 mM imidazole, 1 mM DTT, and 5% glycerol). Bound proteins were eluted with 1 CV of
93 elution buffer (20 mM NaPi (pH 7.5), 30 mM NaCl, 300 mM imidazole, 1 mM DTT, and 5%
94 glycerol).

95 Eluates were immediately loaded onto a 5 mL HiTrap Heparin HP column (GE Healthcare,
96 Chicago, IL, USA) that was equilibrated with 20 mM HEPES (pH 7.5), 30 mM NaCl, 5 mM TCEP,
97 and 5% glycerol using an AKTA Start FPLC system (GE Healthcare). The column was washed
98 with 10 CV of the equilibration buffer, and the protein was eluted with 20 mM HEPES (pH 7.5),
99 1 M NaCl, 5 mM TCEP, and 5% glycerol over a 50 mL linear gradient in 2 mL fractions. Elution
100 fractions were analyzed by SDS-PAGE, pooled, and dialyzed into storage buffer (20 mM HEPES
101 pH 7.5, 150 mM KCl, 5 mM TCEP, and 20% glycerol) using 3500 MWCO tubing (ThermoFisher).
102 After three buffer exchanges, proteins were flash-frozen in liquid nitrogen and stored at -80 °C.
103 Protein concentrations were measured with a NanoDrop One C spectrophotometer (ThermoFisher)
104 using the molar extinction coefficients listed in Table 1.

105

106 **Table 1.** Amino acid sequences of BRCA1 DBD1, DBD2, and BRCT.

Name	Sequence (N→C)	Molar Extinction Coefficient ($M^{-1}cm^{-1}$)
6xHis-BRCT (aa1646-1861)	HHHHHHENLYFQGVNKRMSMVVSGLTPEEFMLV YKFARKHHITLTNLITEETTHVVMKTDAEFVCERT LKYFLGIAGGKWVVSYFWVTQSIKERKMLNEHD FEVRGDVVNGRNHQGPKRARESQDRKIFRGLEIC CYGPFTNMPTDQLEWMVQLCGASVVKELSSFTL GTGVHPIVVVQPDAWTEDNGFHAIGQMCEAPVV TREWVLDSVALYQCQELDTYLIPQIPHS	39,420
6xHis-DBD1 (aa330-554)	HHHHHHENLYFQGDRRTPSTEKKVDLNADPLCE RKEWNKQKLPCSENPRDTEDVPWITLNSSIQKVN EWFSRSDELLGSDDSHDGESESNAKVADVLDVLN EVDEYSGSSEKIDLLASDPHEALICKSERVHSKSV ESNIEDKIFGKTYRKKASLPNLSHVTENLIIGAFVT EPQIIQERPLTNKLKRKRRPTSGLHPEDFIKKADLA VQKTPEMINQGTNQTEQNGQVMNITNSGHE	20,970
6xHist-DBD2 (aa894-1057)	HHHHHHENLYFQGKQSPKVTFECEQKEENQGKN ESNIKPVQTVNITAGFPVVGQKDKPVDNAKCSIKG	2,980

GSRFCLSSQFRGNETGLITPNKHGLLQNPYRIPPLF

PISFVKTKCKKNLLEEFEEHSMSPEREMGNENIPST

VSTISRNNIRENVFKEASSSNINEVGSSTNEVGSS

107

108 **DNA oligos.** All oligonucleotides were synthesized by Integrated DNA Technologies (IDT;
109 Coralville, IA, USA). Oligos were dissolved in Buffer H (20 mM HEPES pH 7.5, 150 mM KCl, 5
110 mM TCEP, and 5% glycerol), and DNA concentrations were determined spectrophotometrically.
111 Double-stranded DNA was prepared by mixing the non-biotinylated complementary strand in
112 1.05x molar excess over the biotinylated oligo, incubating the sample at 95 °C for 10 minutes, and
113 cooling it slowly to room temperature over 6 hours. A Cy3 label was included in the
114 complementary strand to confirm successful annealing by gel electrophoresis.

115 **Biolayer interferometry (BLI).** BLI assays were performed on a BLItz instrument (Sartorius) in
116 Buffer H at 25 °C. High precision streptavidin-coated biosensors (SAX) were purchased from
117 Sartorius and hydrated in Buffer H for 10 minutes prior to use. For each experiment, the sensor
118 was placed in Buffer H for 30 seconds to collect an initial baseline. Next, 150 nM of biotinylated
119 DNA was loaded onto the sensor over 120 seconds and a second baseline was collected in Buffer
120 H for 30 seconds. Protein samples were then introduced at different concentrations. The
121 association reactions were monitored for 180 seconds, and dissociation of the complexes were
122 examined for 120 seconds in Buffer H. A reference curve was obtained in buffer alone and was
123 subtracted from the other traces. BLI measurements were performed in triplicates on separate days.
124 For further methodological details, see reference (48).

125 **Data analysis.** BLI binding isotherms were constructed by plotting the steady-state response (Δλ)
126 values against protein concentration. The curves were fit to a 1:1 binding model in Scientist 3.0
127 software (Micromath; St. Louis, MO) using the following implicit formulas, where Δλ was the
128 observed signal change, A was the amplitude, and K was the equilibrium association constant. D_f
129 and D_t were the free and total concentration of DNA, while P_f and P_t described the free and total
130 concentration of the protein. The binding constants reported were determined from the average
131 and 95% confidence interval of three independent data sets.

132 $$\Delta\lambda = A\left(\frac{KP_f}{1 + KP_f}\right)$$

133 $$D_t = D_f\left(1 + KP_f\right)$$

134 $$P_t = P_f\left(1 + KD_f\right)$$

135 **RESULTS**

136 **Expression and purification of BRCA1 DNA binding domains**. Recombinant BRCA1 DBD1
137 (aa 330-554), DBD2 (aa 894-1057), and BRCT domain (aa 1646-1861) were expressed in *E. coli*
138 and purified to near homogeneity using Ni-NTA and heparin affinity chromatography. All three
139 proteins migrated as single bands at their expected molecular weights by SDS-PAGE (Figure 1).

140 **Design of DNA substrates**. To examine the DNA binding properties of the BRCA1 domains, we
141 designed three biotinylated DNA substrates as shown in Table 2: a 60 nt ssDNA, a fully annealed
142 blunt-end dsDNA, and a G4 formed from the human telomeric repeat sequence. The ssDNA and
143 dsDNA structures are common repair intermediates in homologous recombination, while the
144 human telomeric G4 was examined due to BRCA1's role in telomere maintenance (28, 29).

145 Branched DNA substrates were excluded maintain 1:1 binding stoichiometry for quantitative
146 analysis of the affinity values.

147 **Table 2.** DNA oligo sequences

Name	Sequence (5'→3')	Molar Extinction Coefficient ($M^{-1}cm^{-1}$)	Molecular Weight (g/mol)
Bioss60R	/5Biosg/CCATGGCTCCTGAGCTAGCTGCAGTAGCCTAAAGGATGAAACTAGGATCTTATGCTCCAT	574,200	18,459
BioG4Telo	/5Biosg/TTAGGGTTAGGGTTAGGGTTAGGG	244,600	7,575
ss60RC	/5Cy3/ATGGAGCATAAGATCCTAGTTTCATCCTTTAGGCTACTGCAGCTAGCTCAGGAGCCATGG	582,700	18,996
Biods60R	Bioss60R + ss60RC		37,849

148

149 **Biolayer interferometry assays**. Biolayer interferometry (BLI) was used to measure the binding
150 affinities of DBD1, DBD2, and BRCT for each DNA substrate. Figure 2A outlines a standard BLI
151 workflow. The streptavidin-coated BLI sensors (SAX) were hydrated in Buffer G, and an initial
152 baseline signal was measured (Phase 1). The biotinylated DNA was loaded onto the SAX

153 biosensors, producing an increase in binding signal (Δλ) (Phase 2). After loading the DNA, the
154 sensor tip was washed in Buffer G to establish a new baseline (Phase 3). This step ensured that the
155 DNA substrate remain bound to the SAX sensors. The proteins were then added at varying
156 concentrations to initiate the association reactions (Phase 4). After reaching a steady-state plateau,
157 the sensor was placed into Buffer G to monitor the dissociation reactions (Phase 5). Figure 2B
158 illustrates the association and dissociation time-courses collected from multiple protein
159 concentrations. The plateau values were plotted against protein concentration and fit to a 1:1
160 interaction model using non-linear least squares analysis to determine the equilibrium constant (K)
161 values (Figure 2C).

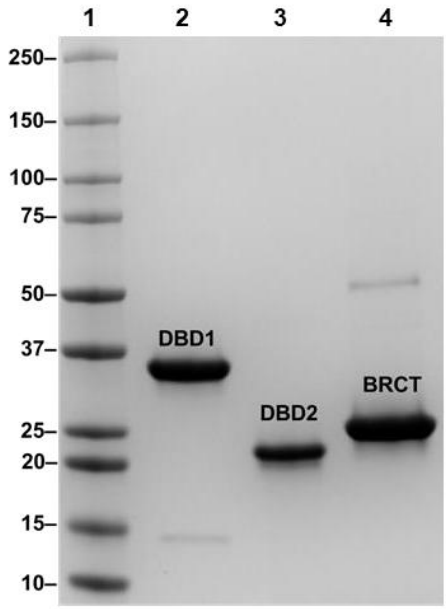

162

163 **Figure 1.** SDS-PAGE of purified recombinant BRCA1 DBD1, DBD2, and BRCT. A protein
164 ladder with known molecular weights (kDa) was loaded into Lane 1. Purified DBD1 (Lane 2),
165 DBD2 (Lane 3), and BRCT (Lane 4) were loaded in the respective lanes.

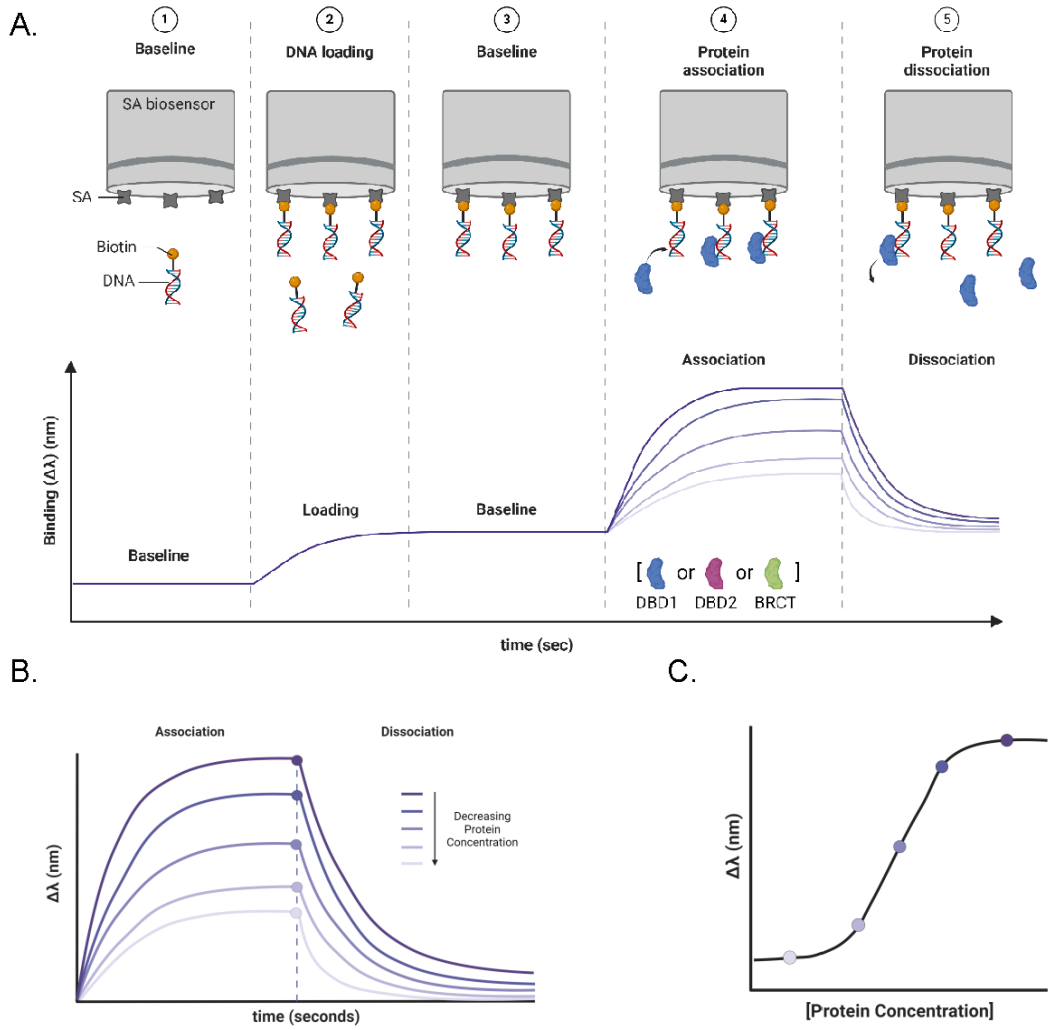

Figure 2. Biolayer interferometry (BLI) binding assays. **A.** Cartoon depicting a time-course of each step of a BLI experiment. The interference pattern of a streptavidin-coated (SAX) biosensor was measured in Buffer G to establish a baseline (Phase 1). Biotinylated DNA was loaded onto the sensor tip through biotin-SA interactions and an increase in Δλ was measured (Phase 2). The biosensor was washed with buffer to confirm the DNA substrate remained surface-immobilized and to establish a new baseline (Phase 3). Protein (DBD1, blue; DBD2, magenta; BRCT, green) was introduced to initiate the association reaction (Phase 4). Once a binding equilibrium was

174 reached, the biosensor was returned to Buffer G to examine the dissociation of the protein-DNA
175 complexes (Phase 5).

176 **DNA binding profiles of the BRCA1 domains**. Quantitative BLI revealed distinct DNA substrate
177 preferences for each BRCA1 domain. DBD1 exhibited the highest binding affinity for dsDNA (K
178 = 2.92 ± 0.66 x 10^7 M^{-1}; K_D = 3.55 ± 0.90 x 10^{-8} M), followed by a lower affinity for ssDNA (K =
179 1.67 ± 0.65 x 10^7; K_D = 6.84 ± 3.38 x 10^{-8} M), and the weakest affinity for G4 DNA (K =
180 1.52 ± 0.28 x 10^7 M^{-1}; K_D = 6.72 ± 1.25 x 10^{-8} M) (Figure 3). This preference for dsDNA is
181 consistent with the potential role of DBD1 in recognizing DSB during early HR. Although DBD1
182 showed measurable binding to ssDNA and to G4 DNA, these interactions were weaker, indicating
183 lower selectivity for these repair intermediates.

184 DBD2 showed the opposite binding pattern, with the highest affinity for G4 DNA (K = 3.26 ± 1.21
185 x 10^7 M^{-1}; K_D = 3.47 ± 1.61 x 10^{-8} M), followed by ssDNA (K = 2.47 ± 0.23 x 10^7 M^{-1}; K_D = 4.08
186 ± 0.37 x 10^{-8} M), and the weakest binding to dsDNA (K = 2.27 ± 0.31 x 10^7 M^{-1}; K_D = 4.46 ± 0.60
187 x 10^{-8} M) (Figure 4). The enhanced preference for G4 structures suggests that DBD2 may
188 contribute to BRCA1's established role in resolving secondary structures at telomeres or fragile
189 sites under replication stress.

190 The BRCT, although traditionally described as a phosphopeptide-binding domain, also
191 demonstrated detectable binding to DNA substrates with the same affinity patterns as DBD2. The
192 BRCT bound strongest to G4 DNA (K = 6.82 ± 1.09 x 10^6 M^{-1}; K_D = 1.49 ± 0.26 x 10^{-7} M),
193 followed closely by ssDNA (K = 6.34 ± 0.49 x 10^6 M^{-1}; K_D = 1.58 ± 0.12 x 10^{-7} M), and the
194 weakest binding to dsDNA (K = 5.46 ± 0.42 x 10^6 M^{-1}; K_D = 1.84 ± 0.14 x 10^{-7} M) (Figure 5).

Notably, these affinity values were ~10-fold lower than those observed for DBD2. All BLI binding results are summarized in Table 3.

Figure 3. Plots of BRCA1 DBD1. **A.** ssDNA. **B.** dsDNA. **C.** G4 DNA.

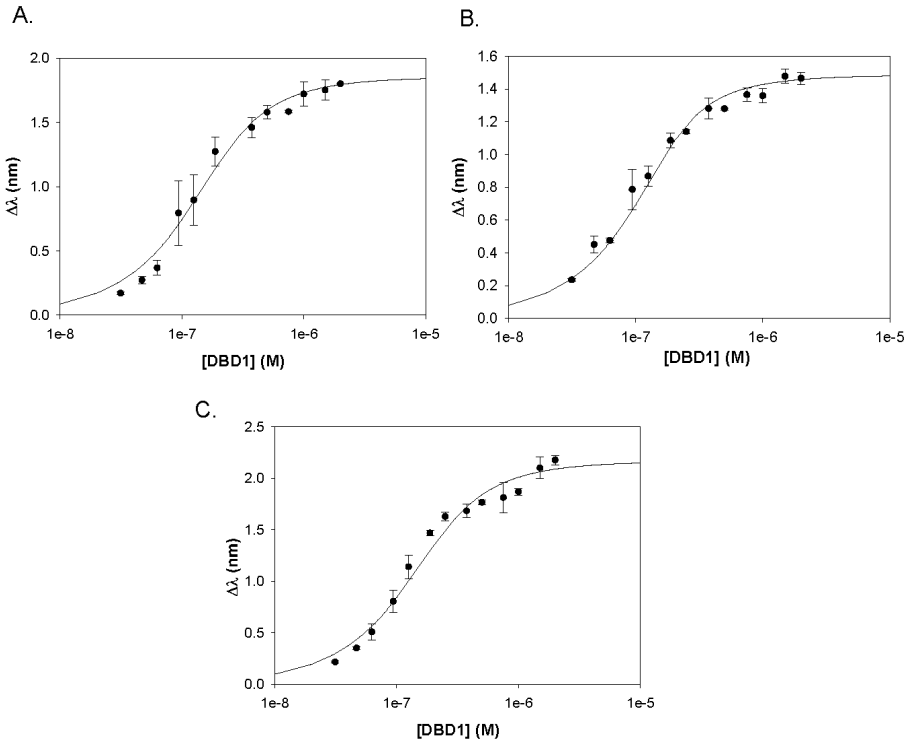

Figure 4. Plots of BRCA1 DBD2. **A.** ssDNA. **B.** dsDNA. **C.** G4 DNA.

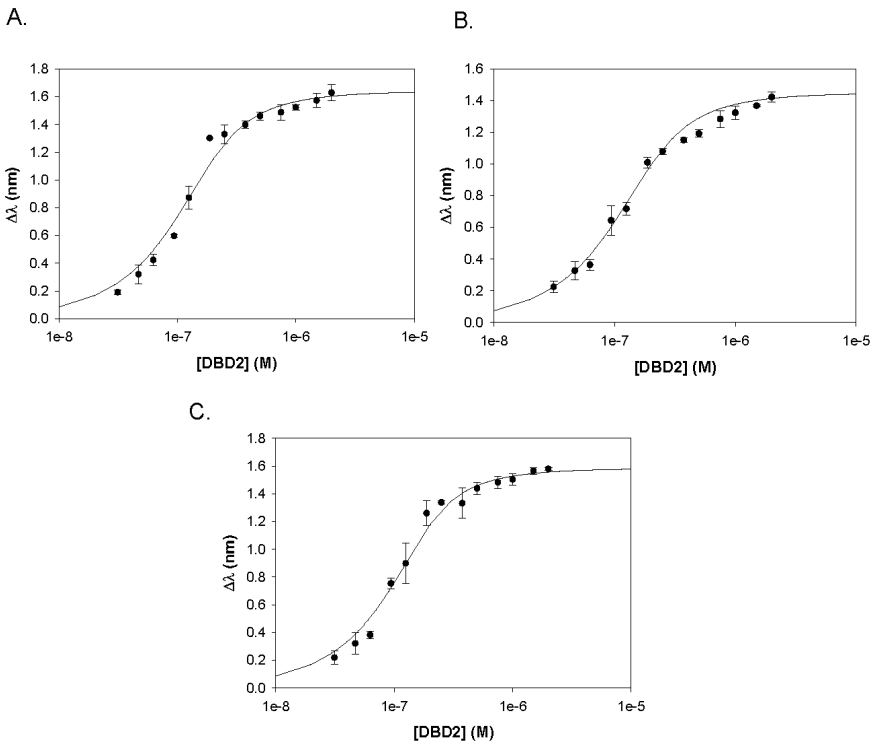

Figure 5. Plots of BRCA1 BRCT. **A**. ssDNA. **B.** dsDNA. **C.** G4 DNA.

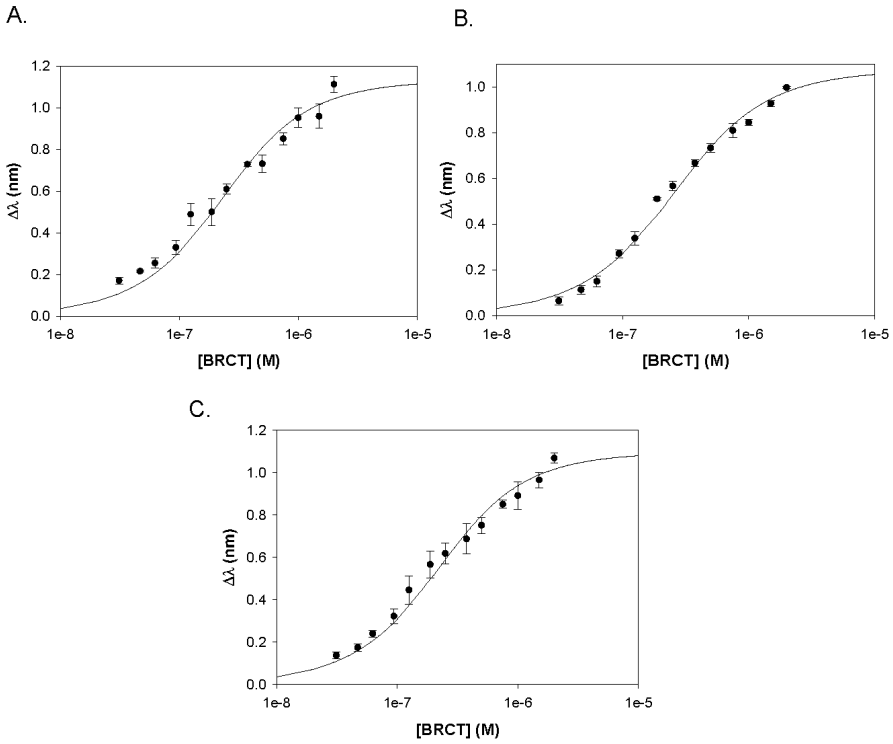

Table 3. Summary of BLI data

Protein	DNA Substrate	K (M^{-1})	K_D (M)	A	R^2
DBD1	ssDNA	$1.67 \pm 0.65 \times 10^{7}$	$6.84 \pm 3.38 \times 10^{-8}$	1.85 ± 0.037	0.995
	G4	$1.52 \pm 0.28 \times 10^{7}$	$6.72 \pm 1.25 \times 10^{-8}$	2.16 ± 0.044	0.995
	dsDNA	$2.92 \pm 0.66 \times 10^{7}$	$3.55 \pm 0.90 \times 10^{-8}$	1.48 ± 0.021	0.997
DBD2	ssDNA	$2.47 \pm 0.23 \times 10^{7}$	$4.08 \pm 0.37 \times 10^{-8}$	1.64 ± 0.029	0.996
	G4	$3.26 \pm 1.21 \times 10^{7}$	$3.47 \pm 1.61 \times 10^{-8}$	1.58 ± 0.023	0.997
	dsDNA	$2.27 \pm 0.31 \times 10^{7}$	$4.46 \pm 0.60 \times 10^{-8}$	1.45 ± 0.043	0.996
BRCT	ssDNA	$6.34 \pm 0.49 \times 10^{6}$	$1.58 \pm 0.12 \times 10^{-7}$	1.13 ± 0.027	0.993
	G4	$6.82 \pm 1.09 \times 10^{6}$	$1.49 \pm 0.26 \times 10^{-7}$	1.09 ± 0.021	0.995
	dsDNA	$5.46 \pm 0.42 \times 10^{6}$	$1.84 \pm 0.14 \times 10^{-7}$	1.07 ± 0.016	0.997

DISCUSSION

The BRCA1 central DNA binding domain (DBD) has been implicated in recognizing DNA structures that are critical to different repair pathways, including cruciform, supercoiled, G4, and triplex DNA (23, 26, 46, 47). However, definitions of the domain's boundaries have varied. Paull

209 et al. originally characterized the DBD as spanning residues 452–1079, while Brázda et al. refined
210 this to aa 444–1057 (26), and Masuda et al. focused on aa 421–701 (25). Later studies suggested
211 further subdivision—Mark et al. proposed two discrete subdomains (aa 498–663 and 936–1057),
212 while Naseem et al. and Brázda et al. isolated minimal fragments (aa 340–554 and 894–1057,
213 respectively) with DNA binding activity (44, 47, 49). Based on these studies, we generated
214 BRCA1 constructs DBD1 (aa 330-554) and DBD2 (aa 894-1057) to clarify the specific DNA
215 substrate preferences of these domains.

216 In addition, we examined the BRCT domain (aa 1646-1861), a structured phosphoprotein-binding
217 domain with emerging roles in DNA and chromatin interactions (50). While BRCT has been
218 studied extensively in the context of protein-protein interactions, its direct contributions to DNA
219 binding remained less defined. Importantly, prior studies did not provide DNA binding affinity
220 values of the isolated BRCA1 domains, nor did they assess whether the individual domains acted
221 independently or synergistically to engage specific DNA targets.

222 Using BLI, we found that DBD1 preferentially binds to dsDNA with highest affinity, followed by
223 ssDNA and G4 DNA. In contrast, DBD2 and BRCT both exhibited strongest binding to G4 DNA,
224 intermediate binding to ssDNA, and the weakest binding to dsDNA. These findings reflect a
225 functional division of labor among the BRCA1 domains and suggest specialization to form distinct
226 repair intermediates. The 1:1 stoichiometry observed in our BLI experiments supports a model in
227 which these domains engage with DNA substrates directly and independently. DBD1's preference
228 for dsDNA implies a primary role in early HR, potentially acting during the recognition of the
229 blunt DSB ends and the recruitment of nucleases for end resection (7-11). DBD2's preference for
230 G4 DNA is consistent with previous reports linking BRCA1 to the resolution of replication stress
231 and telomeric structures, where G4 DNA commonly form (28, 29). Interestingly, BRCT's lower

232 but selective affinity for G4 and ssDNA supports its proposed role in chromatin remodeling and
233 transcriptional regulation at G4-prone loci (41,43).

234 These binding preferences are further supported by structural models. As shown in Figure 6, DBD1
235 and DBD2 are predicted to occupy opposite, solvent-accessible surfaces of BRCA1, consistent
236 with functional specialization. DBD1 is more surface-exposed and is likely accessible to dsDNA
237 at DSB sites. DBD2 and BRCT, on the other hand, are colocalized on the same surface and may
238 coordinate binding to non-canonical B-form DNA such as G4 structures at the telomeres and
239 chromatin. Since the BRCT is positioned internally within the full-length BRCA1 model, it will
240 have less access to the DNA and thus has lower binding affinities compared to the DBD. DBD2
241 and BRCT may function together in binding to their DNA targets due to their similar positioning
242 on the left-most side of the model. A potential explanation for the difference in binding preferences
243 is that the domains undergo structural changes when bound to DNA. DBD1 and DBD2 are
244 primarily unstructured domains, while BRCT is composed of α helix and β sheets (51). However,
245 circular dichroism studies (see Supporting Information) observed no significant changes in
246 secondary structure contact when any of the domains were bound to DNA. It remains possible that
247 the full-length BRCA1 protein undergoes large-scale conformational rearrangements to
248 accommodate or stabilize binding to specific DNA structures, particularly within multiprotein
249 complexes.

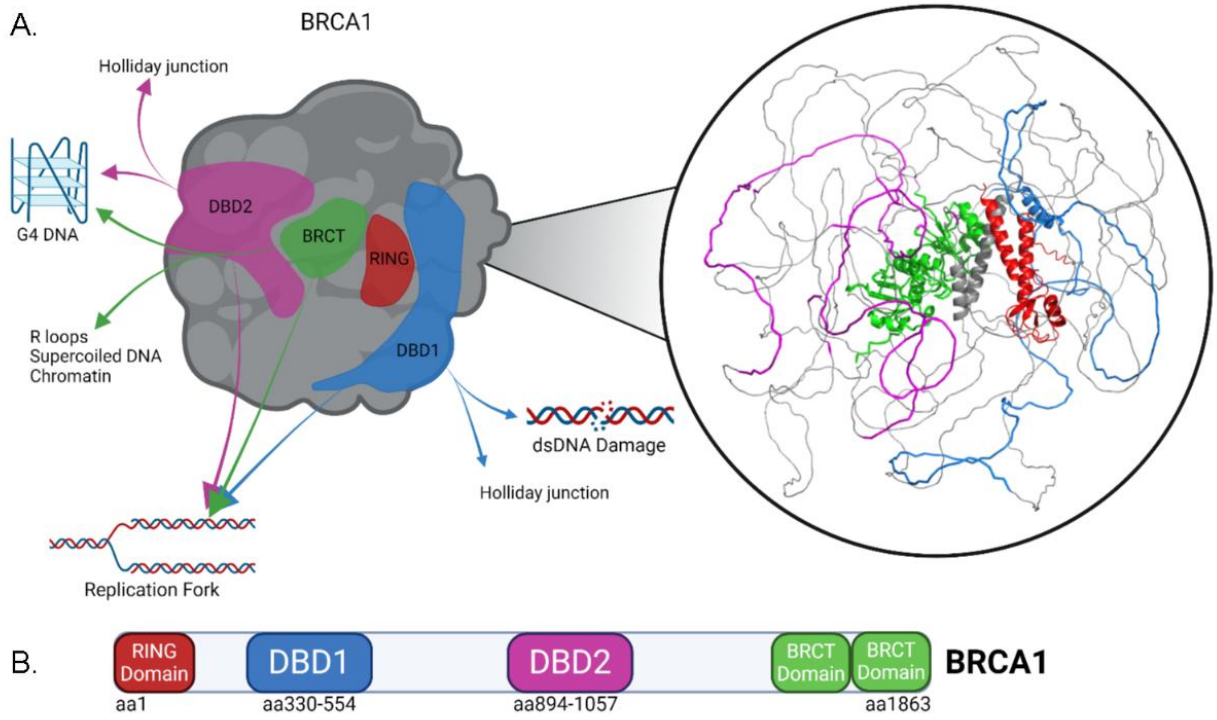

Figure 6. Models and map of BRCA1. **A.** Structural prediction of full-length BRCA1 using AlphaFold2 (right). Cartoon model (left) depicts the preferences of the different regions within BRCA1 in binding to distinct DNA structures. **B.** Cartoon map of BRCA1, highlighting domains RING (aa1-109, red), DBD1 (aa330-554, blue), DBD2 (aa894-1057, magenta), and the tandem BRCT repeats (aa1646-1863, green).

Our results both confirm and refine prior findings. For example, Masuda et al. observed that residues 421–701 prefer dsDNA over ssDNA (25), aligning with the behavior of our DBD1 construct (aa 330–554), which overlaps this region. In contrast, Sturdy et al. reported that aa

259 230–534 preferentially bind four-way junctions (46), which may reflect DBD1 recognizing each
260 arm of the cruciform as individual dsDNA sites. This highlights the importance of substrate
261 design when interpreting DNA binding profiles. Similarly, the broader DBD2-containing
262 fragment (aa 444–1057) used by Brázda et al. exhibited strong binding to G4 and cruciform
263 DNA, a trend preserved in our DBD2 construct (26). These comparisons suggest that DBD2 is
264 the primary determinant of BRCA1's affinity for non-canonical DNA structures, even within
265 larger central constructs. We also observed BRCT binding to dsDNA, consistent with studies by
266 Yamane et al. and Matsumoto et al. (43, 52), and further support the model proposed by Hu et al.
267 in which BRCT contributes to chromatin remodeling at telomeres (41). Given that our G4 was
268 derived from human telomeric repeat sequences, the BRCT's interactions with this substrate
269 further suggests BRCA1's involvement in telomeric surveillance.

270

271 **CONCLUSIONS**

272 Our findings provide quantitative evidence that the BRCA1 DBD exhibit distinct substrate
273 preferences, with DBD1 favoring dsDNA and DBD2 and BRCT preferentially targeting G4 and
274 ssDNA. These data support a functional model in which BRCA1 is guided to specific genomic
275 sites based on domain-specific recognition of DNA structure—DBD1 facilitates BRCA1's
276 recruitment to DSB during early stages of HR; DBD2 and BRCT together enable BRCA1
277 localization to G4-rich regions such as telomeres or stalled replication forks, where BRCA1
278 helps coordinate chromatin remodeling and replication restart. Further studies are needed to
279 determine whether the DBD1-2 fusion (aa 330-1057) exhibits additive or cooperative binding
280 behavior and whether pathogenic BRCA1 variants within these domains alter DNA binding

affinity or substrate specificity. A detailed understanding of these BRCA1-DNA interactions may clarify how specific mutations contribute to cancer risk and guide interpretation of variants of unknown significance (VUS) in clinical studies.

ASSOCIATED CONTENT

Supporting Information

The following files are available free of charge.

Circular dichroism (CD) spectroscopy data (PDF)

ACCESSION CODES

BRCA1, UniProt: P38398

AUTHOR INFORMATION

Corresponding Author

Colin G. Wu; Email: colinwu@oakland.edu

Present Addresses

† K.L.: Wayne State University, Detroit, MI, 48202, USA

§ L.C.: University of Wisconsin-Madison, Madison, WI, 53706, USA

Author Contributions

C.G.W. designed experiments. K.L., L.C., and C.G.W. acquired data and interpreted results. K.L., L.C., E.C., and C.G.W. prepared the manuscript draft. All authors have given approval to the final version of the manuscript.

Funding Sources

This work was supported by AHA grant 19AIREA34460026 to C.G.W.

ACKNOWLEDGMENT

Figures 2 and 6, as well as the abstract graphic, were created with BioRender.com. We thank the Spies Lab for providing the BRCA1 BRCT construct.

ABBREVIATIONS

BRCA1, breast cancer susceptibility gene 1; HR, homologous recombination; DSB, double-strand break; DBD, DNA binding domain; aa, amino acid; BRCT, BRCA1 C-terminal repeats; ssDNA or Bioss60R, single-stranded DNA; dsDNA or Biods60R-Cy3, blunt-end double-stranded DNA; G4 DNA or BioG4Telo, G-quadruplex DNA; 53BP1, tumor suppressor p53-binding protein 1; PALB2, partner and localizer of BRCA2; BRCA2, breast cancer type 2 susceptibility protein; RAD51, DNA repair protein RAD51 homolog 1; NHEJ, non-homologous end-joining; RING, really interesting new gene finger domain; FANCJ, Fanconi anemia complementation group J; BLI, biolayer interferometry; SA, streptavidin

REFERENCES

1. Wu, J.; Lu, L.-Y.; Yu, X., The role of BRCA1 in DNA damage response. *Protein Cell* **2010,** *1* (2), 117-123.

2. Rosen, E. M., BRCA1 in the DNA damage response and at telomeres. *Front. Genet.* **2013,** *4* (85).

324 3. Zhao, W.; Wiese, C.; Kwon, Y.; Hromas, R.; Sung, P., The BRCA Tumor Suppressor
325 Network in Chromosome Damage Repair by Homologous Recombination. *Annu. Rev.*
326 *Biochem.* **2019,** *88*, 221-245.

327 4. Ballal, R. D.; Saha, T.; Fan, S.; Haddad, B. R.; Rosen, E. M., BRCA1 Localization to the
328 Telomere and Its Loss from the Telomere in Response to DNA Damage. *J. Biol. Chem.*
329 **2009,** *284* (52), 36083-36098.

330 5. King, M.-C.; Marks, J. H.; Mandell, J. B.; New York Breast Cancer Study Group, Breast
331 and Ovarian Cancer Risks Due to Inherited Mutations in BRCA1 and BRCA2. *Science*
332 **2003,** *302* (5645), 643-646.

333 6. Nikfarjam, S.; Singh, K. K., DNA damage response signaling: A common link between
334 cancer and cardiovascular diseases. *Cancer Med.* **2022,** *12* (4), 4380-4404.

335 7. Daley, J. M.; Sung, P., 53BP1, BRCA1, and the Choice between Recombination and End
336 Joining at DNA Double-Strand Breaks. *Mol. Cell. Biol.* **2023,** *34* (8), 1380-1388.

337 8. Ceccaldi, R.; Rondinelli, B.; D'Andrea, A. D., Repair Pathway Choices and Consequences
338 at the Double-Strand Break. *Trends Cell Biol.* **2016,** *26* (1), 52-64.

339 9. Sy, S. M. H.; Huen, M. S. Y.; Chen, J., PALB2 is an integral component of the BRCA
340 complex required for homologous recombination repair. *Proc. Natl. Acad. Sci. U. S. A.*
341 **2009,** *106* (17), 7155-7160.

342 10. Zhang, F.; Ma, J.; Wu, J.; Ye, L.; Cai, H.; Xia, B.; Xiaochun, Y., PALB2 Links BRCA1
343 and BRCA2 in the DNA-Damage Response. *Curr. Biol.* **2009,** *19* (6), 524-529.

344 11. Zhang, F.; Fan, Q.; Ren, K.; Andreassen, P. R., PALB2 Functionally Connects the Breast
345 Cancer Susceptibility Proteins BRCA1 and BRCA2. *Mol. Cancer Res.* **2009,** *7* (7).

346 12. Chaudhuri, A. R.; Callen, E.; Ding, X.; Gogola, E.; Duarte, A. A.; Lee, J.-E.; Wong, N.;
347 Lafarga, V.; Calvo, J. A.; Panzarino, N. J.; et al., Replication fork stability confers
348 chemoresistance in BRCA-deficient cells. *Nature* **2016,** *535*, 382-387.

349 13. Xu, Y.; Ning, S.; Wei, Z.; Xu, R.; Xu, X.; Xing, M.; Guo, R.; Xu, D., 53BP1 and BRCA1
350 control pathway choice for stalled replication restart. *eLife* **2017,** *6*.

351 14. Zeman, M. K.; Cimprich, K. A., Causes and consequences of replication stress. *Nat. Cell*
352 *Biol.* **2014,** *16* (1), 2-9.

353 15. Cortez, D., Preventing replication fork collapse to maintain genome integrity. *DNA Repair*
354 **2015,** *32*, 149-157.

355 16. Li, M. L.; Greenberg, R. A., Links between genome integrity and BRCA1 tumor
356 suppression. *Trends Biochem. Sci.* **2012,** *37* (10), 418-424.

357 17. Kass, E. M.; Moynahan, M. E.; Jasin, M., When Genome Maintenance Goes Badly Awry.
358 *Mol. Cell* **2016,** *62* (5), 777-787.

359 18. Daley, J. M.; Niu, H.; Miller, A. S.; Sung, P., Biochemical mechanism of DSB end
360 resection and its regulation. *DNA Repair* **2015,** *32*, 66-74.

361 19. Verma, P.; Greenberg, R. A., Noncanonical views of homology-directed DNA repair.
362 *Genes Dev.* **2016,** *30* (10), 1138-1154.

363 20. Filippo, J. S.; Sung, P.; Klein, H., Mechanism of Eukaryotic Homologous Recombination.
364 *Annu. Rev. Biochem.* **2008,** *77*, 229-257.

365 21. Rickman, K.; Smogorzewska, A., Advances in understanding DNA processing and
366 protection at stalled replication forks. *J. Cell Biol.* **2019,** *218* (4), 1096-1107.

367 22. Bansal, A.; Kaushik, S.; Kukreti, S., Non-canonical DNA structures: Diversity and disease
368 association. *Front. Genet.* **2022,** *13*.

369 23. Paull, T. T.; Cortez, D.; Bowers, B.; Elledge, S. J.; Gellert, M., Direct DNA binding by
370 Brca1. *Proc. Natl. Acad. Sci. U. S. A.* **2001,** *98* (11), 6086-6091.

371 24. Zhao, W.; Steinfeld, J. B.; Liang, F.; Chen, X.; Maranon, D. G.; Ma, C. J.; Kwon, Y.; Rao,
372 T.; Wang, W.; Sheng, C.; et al., BRCA1–BARD1 promotes RAD51-mediated homologous
373 DNA pairing. *Nature* **2017,** *550*, 360-365.

374 25. Masuda, T.; Xu, X.; Dimitriadis, E. K.; Lahusen, T.; Deng, C.-X., "DNA Binding Region"
375 of BRCA1 Affects Genetic Stability through modulating the Intra-S-Phase Checkpoint. *Int.*
376 *J. Biol. Sci.* **2016,** *12* (2), 133-143.

377 26. Brázda, V.; Hároníková, L.; Liao, J. C. C.; Fridrichová, H.; Jagelská, E. B., Strong
378 preference of BRCA1 protein to topologically constrained non-B DNA structures. *BMC*
379 *Mol. Biol.* **2016,** *17* (14).

380 27. Zhu, Q.; Pao, G. M.; Huynh, A. M.; Suh, H.; Tonnu, N.; Nederlof, P. M.; Gage, F. H.;
381 Verma, I. M., BRCA1 tumour suppression occurs via heterochromatin-mediated silencing.
382 *Nature* **2011,** *477*, 179-184.

383 28. Zimmer, J.; Tacconi, E. M. C.; Folio, C.; Badie, S.; Porru, M.; Klare, K.; Tumiati, M.;
384 Markkanen, E.; Halder, S.; Ryan, A.; et al., Targeting BRCA1 and BRCA2 Deficiencies
385 with G-Quadruplex-Interacting Compounds. *Mol. Cell* **2016,** *61* (3), 449-460.

386 29. Xu, H.; Di Antonio, M..; McKinney, S.; Mathew, V.; Ho, B.; O'Neil, N. J.; Dos Santos, N.;
387 Silvester, J.; Wei, V.; Garcia, J.; et al., CX-5461 is a DNA G-quadruplex stabilizer with
388 selective lethality in BRCA1/2 deficient tumours. *Nat. Commun.* **2017,** *8*.

389 30. Wu, L. C.; Wang, Z. W.; Tsan, J. T.; Spillman, M. A.; Phung, A.; Xu, X. L.; Yang, M.-C.
390 W.; Hwang, L.-Y.; Bowcok, A. M.; Baer, R., Identification of a RING protein that can
391 interact in vivo with the BRCA1 gene product. *Nat. Genet.* **1996,** *14*, 430-440.

392 31. Hashizume, R.; Fukuda, M.; Maeda, I.; Nishikawa, H.; Oyake, D.; Yabuki, Y.; Ogata, H.;
393 Ohta, T., The RING Heterodimer BRCA1-BARD1 Is a Ubiquitin Ligase Inactivated by a
394 Breast Cancer-derived Mutation. *J. Biol. Chem.* **2001,** *276* (18).

395 32. Chen, A.; Kleiman, F. E.; Manley, J. L.; Ouchi, T.; Pan, Z.-Q., Autoubiquitination of the
396 BRCA1·BARD1 RING Ubiquitin Ligase. *J. Biol. Chem.* **2002,** *277* (24), 22085-22092.

397 33. Tarsounas, M.; Sung, P., The antitumorigenic roles of BRCA1–BARD1 in DNA repair and
398 replication. *Nat. Rev. Mol. Cell Biol.* **2020,** *21*, 284-299.

399 34. Bork, P.; Hofmann, K.; Bucher, P.; Neuwald, A. F.; Altschul, S. F.; Koonin, E. V., A
400 superfamily of conserved domains in DNA damage-responsive cell cycle checkpoint
401 proteins. *FASEB J.* **1997,** *11* (1), 68-76.

402 35. Botuyan, M. V. E.; Nominé, Y.; Yu, X.; Juranic, N.; Macura, S.; Chen, J.; Mer, G.,
403 Structural Basis of BACH1 Phosphopeptide Recognition by BRCA1 Tandem BRCT
404 Domains. *Structure* **2004,** *12* (7), 1137-1146.

405 36. Clapperton, J. A.; Manke, I. A.; Lowery, D. M.; Ho, T.; Haire, L. F.; Yaffe, M. B.;
406 Smerdon, S. J., Structure and mechanism of BRCA1 BRCT domain recognition of
407 phosphorylated BACH1 with implications for cancer. *Nat. Struct. Mol. Biol.* **2004,** *11*, 512-
408 518.

409 37. Shiozaki, E. N.; Gu, L.; Yan, N.; Shi, Y., Structure of the BRCT Repeats of BRCA1 Bound
410 to a BACH1 Phosphopeptide: Implications for Signaling. *Mol. Cell* **2004,** *14* (3), 405-412.

411 38. Wu, C. G.; Spies, M., G-quadruplex recognition and remodeling by the FANCJ helicase
412 *Nucleic Acids Res.* **2016,** *44* (18), 8742-8753.

413 39. Leung, C. C. Y.; Glover, J. N. M., BRCT domains: Easy as one, two, three. *Cell Cycle*
414 **2011,** *10* (15), 2461-2470.

415 40. Rudolph, J.; Muthurajan, U. M.; Palacio, M.; Mahadevan, J.; Roberts, G.; Erbse, A. H.;
416 Dyer, P. N.; Luger, K., The BRCT domain of PARP1 binds intact DNA and mediates
417 intrastrand transfer. *Mol. Cell* **2021,** *81* (24), 4994-5006.e5.

418 41. Hu, Y.-F.; Hao, Z. L.; Li, R., Chromatin remodeling and activation of chromosomal DNA
419 replication by an acidic transcriptional activation domain from BRCA1. *Genes Dev.* **1999,**
420 *13* (6), 637-642.

42. Yamane, K.; Tsuruo, T., Conserved BRCT regions of TopBP1 and of the tumor suppressor BRCA1 bind strand breaks and termini of DNA. *Oncogene* **1999,** *18*, 5194-5203.

43. Chang, C.-W.; Singh, A. K.; Li, M.; Guan, L.; Le, N.; Omabe, K.; Liang, F.; Liu, Y., The BRCA1 BRCT promotes antisense RNA production and double-stranded RNA formation to suppress ribosomal R-loops. *Proc. Natl. Acad. Sci. U. S. A.* **2022,** *119* (50).

44. Mark, W.-Y.; Liao, J. C. C.; Lu, Y.; Ayed, A.; Laister, R.; Szymczyna, B.; Chakrabartty, A.; Arrowsmith, C. H., Characterization of Segments from the Central Region of BRCA1: An Intrinsically Disordered Scaffold for Multiple Protein–Protein and Protein–DNA Interactions? *J. Mol. Biol.* **2005,** *345* (2), 275-287.

45. Naseem, R.; Webb, M., Analysis of the DNA Binding Activity of BRCA1 and Its Modulation by the Tumour Suppressor p53. *PLoS One* **2008,** *3* (6).

46. Sturdy, A.; Naseem, R.; Webb, M., Purification and Characterisation of a Soluble N-terminal Fragment of the Breast Cancer Susceptibility Protein BRCA1. *J. Mol. Biol.* **2004,** *340* (3), 469-475.

47. Brázda, V.; Jagelska, E. B.; Liao, J. C. C.; Arrowsmith, C. H., The Central Region of BRCA1 Binds Preferentially to Supercoiled DNA. *J. Biomol. Struct. Dyn.* **2009,** *27* (1), 97-103.

48. Lowran, K.; Salib, V.; Cismas, E.; Wu, C. G., Advancing the study of protein-G4 interactions in DNA repair: Insights from biolayer interferometry. *Methods in enzymology* **2024,** *695*, 89-101.

441 49. Naseem, R.; Sturdy, A.; Finch, D.; Jowitt, T.; Webb, M., Mapping and conformational
442 characterization of the DNA-binding region of the breast cancer susceptibility protein
443 BRCA1 *Biochem. J.* **2006,** *395* (3), 529-535.

444 50. Peña-Guerrero, J.; Fernández-Rubio, C.; García-Sosa, A. T.; Nguewa, P. A., BRCT
445 Domains: Structure, Functions, and Implications in Disease—New Therapeutic Targets for
446 Innovative Drug Discovery against Infections. *Pharmaceutics* **2023,** *15* (7).

447 51. Williams, R. S.; Green, R.; Glover, J. N. M., Crystal structure of the BRCT repeat region
448 from the breast cancer-associated protein BRCA1. *Nat. Struct. Biol.* **2001,** *8*, 838-842.

449 52. Matsumoto, T.; Go, K.; Hyodo, M.; Koiwai, K.; Maezawa, S.; Hayano, T.; Suzuki, M.;
450 Koiwai, O., BRCT domain of DNA polymerase μ has DNA-binding activity and promotes
451 the DNA polymerization activity. *Genes Cells* **2012,** *17* (9), 790-806.

452 53. Zhang, X.; Moréra, S.; Bates, P. A.; Whitehead, P. C.; Coffer, A. I.; Hainbucher, K.; Nash,
453 R. A.; Sternberg, M. J. E.; Lindahl, T.; Freemont, P. S., Structure of an XRCC1 BRCT
454 domain: a new protein–protein interaction module. EMBO J. **1998**, 17, 6404-6411.

455 54. Pryor, J. M.; Gakhar, L.; Washington, M. T., Structure and functional analysis of the BRCT
456 domain of translesion synthesis DNA polymerase Rev1. Biochemistry **2013**, 52 (1), 254-
457 263.

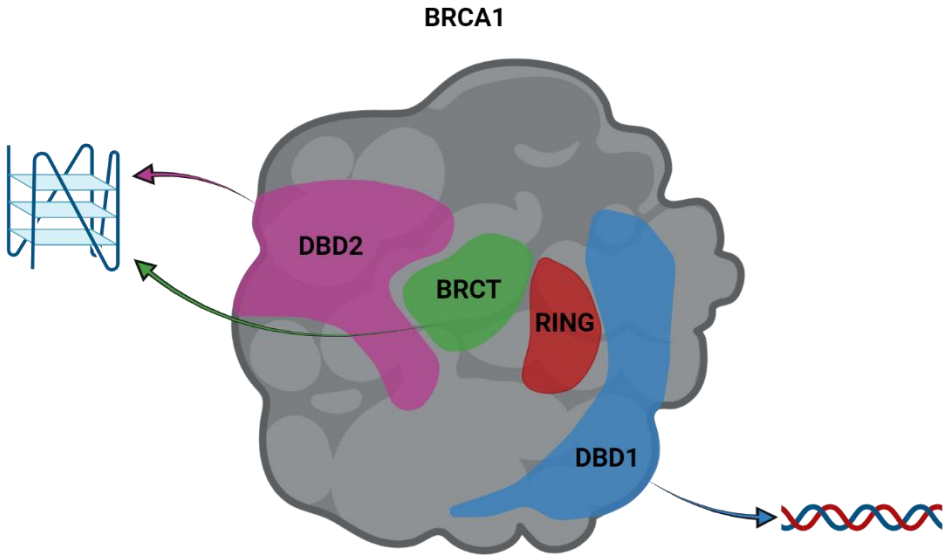

For Table of Contents only.